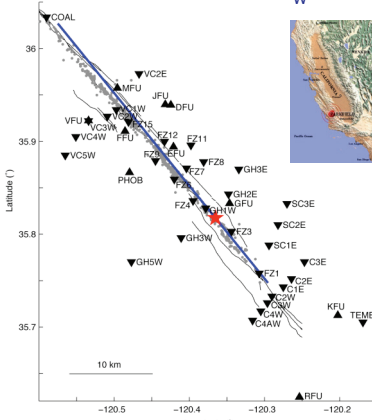


## The 2004 $M_w$ 6.0 Parkfield Earthquake



Parkfield marks the transition between a seismically locked section and a creeping section of the San Andreas Fault (SAF). The locked section, to the SE of Parkfield, is characterized by large earthquakes that occur with a long recurrence interval (last earthquake in 1857 - M<sub>8</sub> Fort Tejon). The creeping section, NW of Parkfield, displays surface creep, as well as very active microseismicity. Bakun and McEvilly (1984) noticed that Parkfield experienced moderate -  $M_{6.6}$  - earthquakes in average every 22 years. They furthermore observed that the waveforms from the 1922, 1934 and 1966 Parkfield earthquakes were similar. Only identical ruptures can produce identical ground-motion. Thus Bakun and McEvilly (1984) proposed that a "characteristic"  $M_{6.6}$  Parkfield earthquake was due before 1993. As a consequence of their prediction, Parkfield became heavily instrumented. The long awaited  $M_{6.6}$  "1993" earthquake occurred on September 28, 2004. It generated the largest amount of near-source data ever. We invert this unique dataset in order to find a rupture model for the earthquake. Velocity structure, conductivity, and drilling, indicate that the Parkfield fault-zone is composed of very heterogeneous material. To reduce noise in the data, we study site effects at the Parkfield array. The 2004 earthquake produced the largest Peak Ground Velocities (PGV) ever observed for a  $M_{6.6}$  event. Site effects explain fairly well the distribution and amplitude of PGVs.

Figure 1. Map of Parkfield with seismic stations used in the inversion. Triangles - USGS stations; Inverted triangles - CGS stations; Red star - epicenter; Gray dots - aftershocks (Hardebeck and Michael, 2004); Blue line - modeled fault projection.

## 2. Site effects inferred from the 1983 Coalinga earthquake

The 1983  $M_{6.5}$  Coalinga thrust earthquake took place approximately 25 km NE of Parkfield. It illuminated identically all the stations in the Parkfield array. We assume that deviations on ground-motion from a common source signal denote site effects.

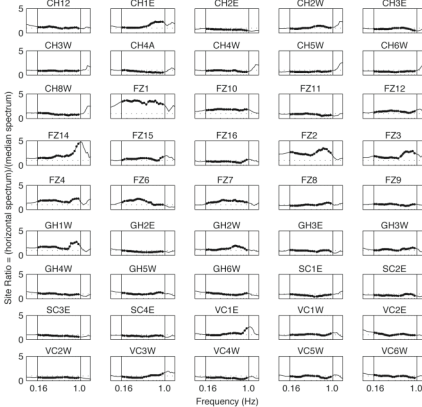
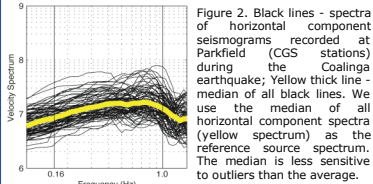


Figure 2. Black lines - spectra of horizontal component seismograms recorded at Parkfield (CGS stations) during the Coalinga earthquake; Yellow thick line - median of all black lines. We use the median of all horizontal component spectra (yellow spectrum) as the reference source spectrum. The median is less sensitive to outliers than the average.

Figure 3. The Site Ratio (SR) is given by the ratio between the horizontal spectrum and the source spectrum. The horizontal spectrum is the average of horizontal component spectra recorded at a given station. We assume that the source spectrum is given by the median of all horizontal component spectra. When  $SR=1$ , we infer that the station is not affected by site effects.  $SR>1$  corresponds to amplification of ground-motion.

## 4. Kinematic model

We account for site effects in two complementary ways: 1) we divide the observed data by the station amplification factor (average of SR); and 2) we downweight stations with large resonances (variance of SR). We furthermore downweight all vertical component data by a factor of 10 in relation to horizontal data.

We use a non-linear annealing algorithm (Liu and Archuleta, 2004) to invert data from 43 three-component strong-motion seismographs. We compute 10 rupture models that explain equally well the data. The 10 models are obtained using the same data and algorithm, but different seeds for random numbers generation (there is a component of randomness in our inversion method).

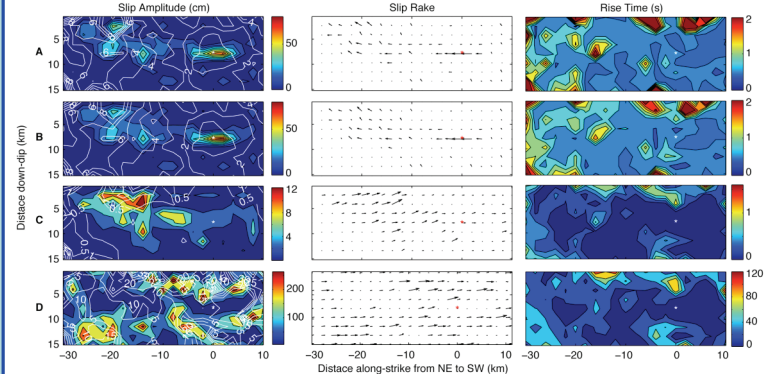


Figure 5. 1<sup>st</sup> column - slip amplitude (cm) and rupture time (white lines are 1 sec contours); 2<sup>nd</sup> column - slip rake; 3<sup>rd</sup> column - rise time (sec). Row A - rupture model with smallest final misfit; Row B - average of 10 rupture models, with similar misfits, obtained with different random seeds; Row C - standard deviation of the 10 models; Row D - coefficient of variance of the 10 models. The white asterisk marks the hypocenter. The coefficient of variance indicates that the areas of small slip are the most poorly resolved. The standard deviation is maximum (12 cm) in a zone of relatively large slip, towards the NW of the hypocenter. We cannot resolve well the details of slip in this. Slip is maximum (65 cm) directly to the SE of the hypocenter. The direction of slip is purely right-lateral close to the hypocenter, and has a component of upward motion towards the NW, at shallow depths. Rise time is not well resolved due to the limited range of frequencies inverted.

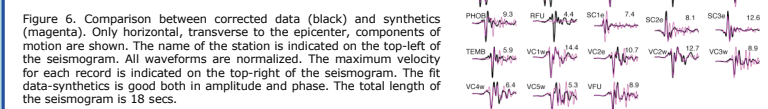
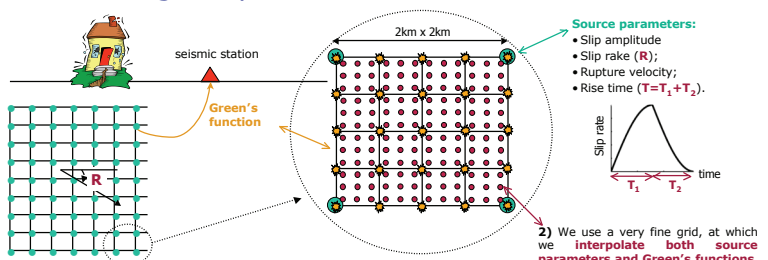


Figure 6. Comparison between corrected data (black) and synthetics (magenta). Only horizontal, transverse to the epicenter, components of motion are shown. The name of the station is indicated on the top-left of the seismogram. All waveforms are normalized. The maximum velocity for each record is indicated on the top-right of the seismogram. The fit data-synthetics is good both in amplitude and phase. The total length of the seismogram is 18 sec.

References  
Bakun, W., and T. McEvilly (1984). Recurrence models and Parkfield, California, earthquakes. *Journal of Geophysical Research*, 89, 3051-3058.  
Liu, P., and R. Archuleta (2004). A new nonlinear finite fault inversion with three-dimensional Green's functions: application to the 1989 Loma Prieta, California, earthquake. *Journal of Geophysical Research*, 109, R02318, doi:10.1029/2003JB002625.  
Hardebeck, J. L., and A. Michael (2004). Earthquake locations before and after the 2004  $M_{6.6}$  Parkfield Earthquake. *Eos Trans. AGU*, 85 (47), Fall Meet. Suppl., Abstract S51C-0170W, 2004.  
Thurber, C. S., R. Aster, W. Roberts, M. Gold, L. Powell, and K. Ritterger (2003). Earthquake locations and three-dimensional fault zone structure along the creeping section of the San Andreas fault near Parkfield, CA, prepared for SAOP. *Geophysical Research Letters*, 30, 3, 1112, doi:10.1029/2002GL016004.  
Bathen-Phillips, D. and A. J. Michael (2005). Three-dimensional velocity structure, seismicity, and fault structure in the Parkfield Region, central California. *J. of Geophys. Res.*, 110, 15373-15378.

The data we used was collected, pre-processed and made available by the California Geological Survey (CGS) and the United States Geological Survey (USGS). A cluster sponsored by Hewlett-Packard at the California NanoSystems Institute (CNSI), UC Santa Barbara, was used for the computations. S. Custodio acknowledges a PhD fellowship from the Portuguese Foundation for Science and Technology. The work was supported by the Southern California Earthquake Center and by the National Science Foundation.

## 1. Obtaining a rupture model - kinematic inversion



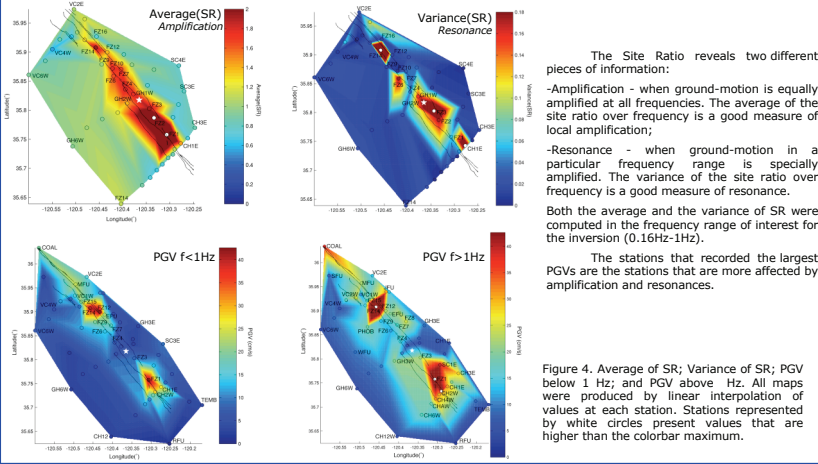
Some assumptions of our model:

- The fault strikes  $141^\circ$  SE and dips  $89^\circ$  SW;
- The rupture was at maximum 40 km long;
- The ruptured area is deeper than 0.5 km (no surface rupture);
- The velocity structure is well approximated by a 1D bilateral model (NE - slow; SW - fast; after Eberhart-Phillips and Michael (1993) and Thurber et al. (2003)).

**3)** We measure the misfit between the computed synthetics and observed data. We compute synthetics for many different sets of source parameters. The goal of our global inversion scheme is to obtain a rupture model that generates synthetics with the smallest misfit to data (Liu and Archuleta, 2004).

Figure 4. Average of SR; Variance of SR; and PGV below 1 Hz; and PGV above 1 Hz. All maps were produced by linear interpolation of values at each station. Stations represented by white circles present values that are higher than the colorbar maximum.

## 3. Site effects and Peak Ground Velocity



The Site Ratio reveals two different pieces of information:

- Amplification - when ground-motion is equally amplified at all frequencies. The average of the site ratio over frequency is a good measure of local amplification;
- Resonance - when ground-motion in a particular frequency range is specially amplified. The variance of the site ratio over frequency is a good measure of resonance.

Both the average and the variance of SR were computed in the frequency range of interest for the inversion (0.16Hz-1Hz).

The stations that recorded the largest PGVs are the stations that are more affected by amplification and resonances.